

## MIT Open Access Articles

*4D dynamic imaging of the eye using ultrahigh speed SS-OCT*

The MIT Faculty has made this article openly available. **Please share** how this access benefits you. Your story matters.

**Citation:** Liu, Jonathan J., Ireneusz Grulkowski, Benjamin Potsaid, Vijaysekhar Jayaraman, Alex E. Cable, Martin F. Kraus, Joachim Hornegger, Jay S. Duker, and James G. Fujimoto. "4D Dynamic Imaging of the Eye Using Ultrahigh Speed SS-OCT." Edited by Fabrice Manns, Per G. Söderberg, and Arthur Ho. Ophthalmic Technologies XXIII (March 26, 2013). © (2013) COPYRIGHT Society of Photo-Optical Instrumentation Engineers (SPIE)

**As Published:** <http://dx.doi.org/10.1117/12.2004369>

**Publisher:** SPIE

**Persistent URL:** <http://hdl.handle.net/1721.1/86411>

**Version:** Final published version: final published article, as it appeared in a journal, conference proceedings, or other formally published context

**Terms of Use:** Article is made available in accordance with the publisher's policy and may be subject to US copyright law. Please refer to the publisher's site for terms of use.



# 4-D dynamic imaging of the eye using ultrahigh speed SS-OCT

Jonathan J. Liu<sup>1</sup>, Ireneusz Grulkowski<sup>1</sup>, Benjamin Potsaid<sup>1,2</sup>, Vijaysekhar Jayaraman<sup>3</sup>, Alex E. Cable<sup>2</sup>, Martin F. Kraus<sup>4</sup>, Joachim Hornegger<sup>4</sup>, Jay S. Duker<sup>5</sup>, and James G. Fujimoto<sup>1</sup>

<sup>1</sup>*Department of Electrical Engineering and Computer Science & Research Laboratory of Electronics, Massachusetts Institute of Technology, Cambridge, MA, USA 02139;*

<sup>2</sup>*Advanced Imaging Group, Thorlabs Inc., Newton, NJ, USA 07860;*

<sup>3</sup>*Praevium Research Inc., Santa Barbara, CA, USA 93111;*

<sup>4</sup>*Pattern Recognition Lab & School of Advanced Optical Technologies, University Erlangen-Nuremberg, Erlangen, Germany 91054;*

<sup>5</sup>*New England Eye Center & Tufts Medical Center, Tufts University, Boston, MA, USA 02116;*

## ABSTRACT

Recent advances in swept-source / Fourier domain optical coherence tomography (SS-OCT) technology enable in vivo ultrahigh speed imaging, offering a promising technique for four-dimensional (4-D) imaging of the eye. Using an ultrahigh speed tunable vertical cavity surface emitting laser (VCSEL) light source based SS-OCT prototype system, we performed imaging of human eye dynamics in four different imaging modes: 1) Pupillary reaction to light at 200,000 axial scans per second and 9  $\mu\text{m}$  resolution in tissue. 2) Anterior eye focusing dynamics at 100,000 axial scans per second and 9  $\mu\text{m}$  resolution in tissue. 3) Tear film break up at 50,000 axial scans per second and 19  $\mu\text{m}$  resolution in tissue. 4) Retinal blood flow at 800,000 axial scans per second and 12  $\mu\text{m}$  resolution in tissue. The combination of tunable ultrahigh speeds and long coherence length of the VCSEL along with the outstanding roll-off performance of SS-OCT makes this technology an ideal tool for time-resolved volumetric imaging of the eye. Visualization and quantitative analysis of 4-D OCT data can potentially provide insight to functional and structural changes in the eye during disease progression. Ultrahigh speed imaging using SS-OCT promises to enable novel 4-D visualization of real-time dynamic processes of the human eye. Furthermore, this non-invasive imaging technology is a promising tool for research to characterize and understand a variety of visual functions.

**Keywords:** 4D, SS-OCT, VCSEL, ophthalmology, pupil, accommodation, tear film, retinal blood flow

## 1. INTRODUCTION

Recent developments in swept-source and spectral domain optical coherence tomography (OCT) technologies have enabled ultrahigh speed OCT imaging at over 100,000 axial scans (A-scans) per second [1-4]. Novel ultralong range and ultrahigh speed imaging of the eye has been demonstrated using SS-OCT with vertical cavity surface emitting laser (VCSEL) technology [5]. In this paper, we demonstrate time resolved volumetric data using four-dimensional (4-D) OCT with speeds up to forty volumes per second. We imaged pupillary reactions, anterior eye focusing dynamics, tear film break up, and retinal blood flow. The real-time dynamics of the human eye is captured and analyzed for characterizing visual functions.

## 2. MATERIALS AND METHODS

We developed a VCSEL light source based prototype SS-OCT system (Figure 1) [5]. The laser was operated in four different modes with center wavelengths at around 1060 nm (Table 1). To image the pupillary reaction, the VCSEL light source was operated at an axial scan rate of 200 kHz with 85 nm tuning range yielding 9  $\mu\text{m}$  resolution and 5.6 mm Nyquist-limited imaging range in tissue. To image anterior eye accommodation dynamics, the axial scan rate was reduced to 100 kHz to achieve a 10.3 mm Nyquist-limited imaging range in tissue. To image tear film break up, the VCSEL light source was operated at a reduced axial scan rate of 50 kHz and reduced 30 nm tuning range for 19  $\mu\text{m}$

resolution and 60 mm Nyquist-limited imaging range in tissue. Finally, to image retinal blood flow, the VCSEL light source was operated at an axial scan rate of 800 kHz and 50 nm tuning range for 12  $\mu\text{m}$  resolution and 2.5mm Nyquist-limited imaging range in tissue. A/D data acquisition cards (ATS9870 & ATS9350; AlazarTech) at either a fixed 1 GSPS or a fixed 500 MSPS sampling rate with dual channel acquisition were used. The incident power on the cornea for all imaging modes was 1.9 mW, within the American National Standard Institute (ANSI) safety limits. Studies were performed under protocols approved by the MIT Committee on the Use of Humans as Experimental Subjects (COUHES) and written consent from participants was obtained.

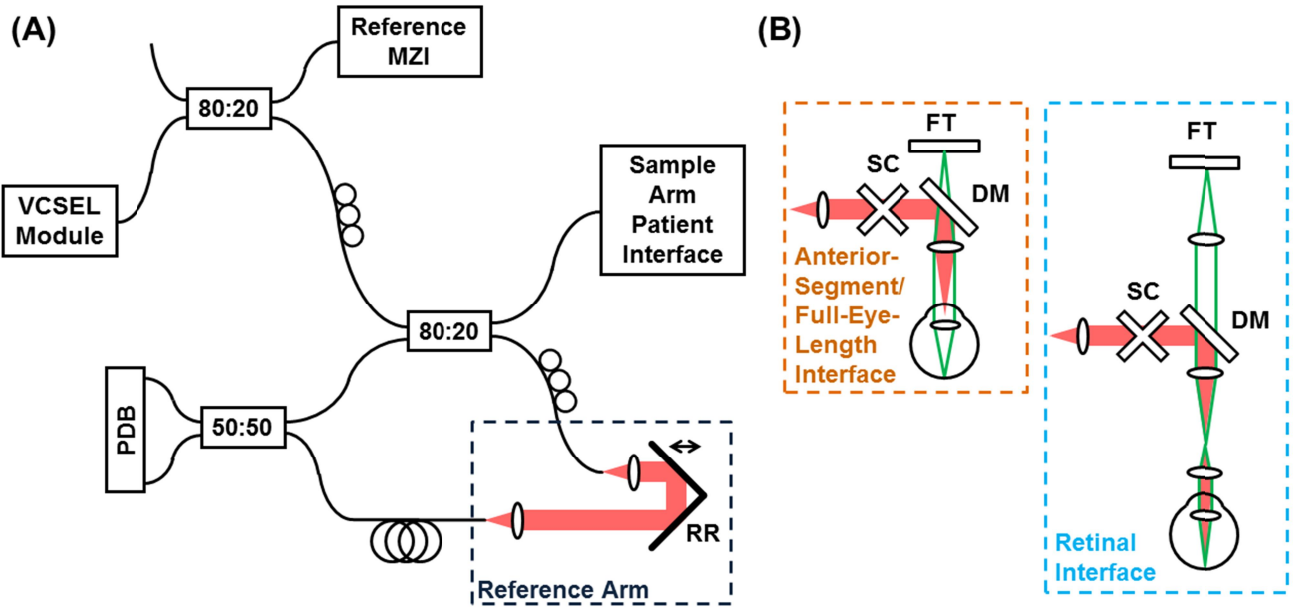


Figure 1. (A) VCSEL based SS-OCT prototype setup. (B) Different interface configurations. Full-eye-length imaging was performed by using a longer focal length lens in the anterior segment configuration. Retinal imaging was performed by adding ocular lens to the anterior segment configuration and adjusting the fixation target path. SC – galvanometric scanners, FT – fixation target, DM – dichroic mirror, DC – dispersion compensation glass, RR – retroreflector, PDB – balanced photodetectors, MZI – Mach-Zehnder interferometer.

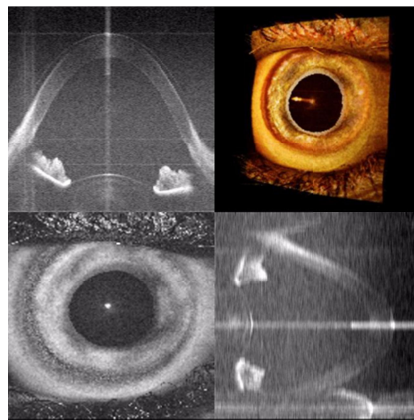
Table 1. Configuration of VCSEL SS-OCT system.

Parameter	Pupillary response	Accommodation	Tear film break up	Retinal blood flow
Effective imaging speed	200,000 A-scans/s	100,000 A-scans/s	50,000 A-scans/s	800,000 A-scans/s
Wavelength tuning range	85 nm	85 nm	30 nm	50 nm
Axial resolution (tissue)	9 $\mu\text{m}$	9 $\mu\text{m}$	19 $\mu\text{m}$	12 $\mu\text{m}$
Sample arm interface	Anterior segment	Anterior segment	Full eye length	Retinal
Transverse resolution	30 $\mu\text{m}$	30 $\mu\text{m}$	73 $\mu\text{m}$	25 $\mu\text{m}$
Acquisition card	ATS9870 (1 GSPS)	ATS9870 (1 GSPS)	ATS9870 (1 GSPS)	ATS9350 (500 MSPS)

### 3. RESULTS AND DISCUSSION

#### 3.1 Pupillary response

The iris is a dynamic structure whose configuration regularly changes in response to light and during accommodation. Dynamic changes in intraocular structures caused by illumination or dilation are suggested to be risk factors for glaucoma development. Studying the dynamic response of the pupil to dark-light stimulus may provide a more comprehensive assessment of risks to primary-angle closure development and may help understand the pathophysiology of angle closure glaucoma [6-8]. We demonstrated 4-D imaging of the pupil response to light stimulus from an LED positioned adjacent to the eye, where sequential 150 x 150 axial-scan volumes over 17 mm x 17 mm were acquired at ~8 volumes per second for 5 seconds with an axial scan rate of 200 kHz enabling the visualization of changes in the iris in time and in three dimensions (Video 1). The pupillary response is shown in Figure 2 where two time points in the 4-D data are displayed. The iris response to light stimulus can be quantitatively analyzed by measuring pupil size/area changes in time. As shown in Figure 2(A), the pupil area decreased drastically when light stimulus was applied. In contrast, the time constant of the pupil diameter recovery was longer than when stimulus was applied.



Video 1. 4-D OCT imaging of the pupillary reflex. <http://dx.doi.org/10.1117/12.2004369.1>

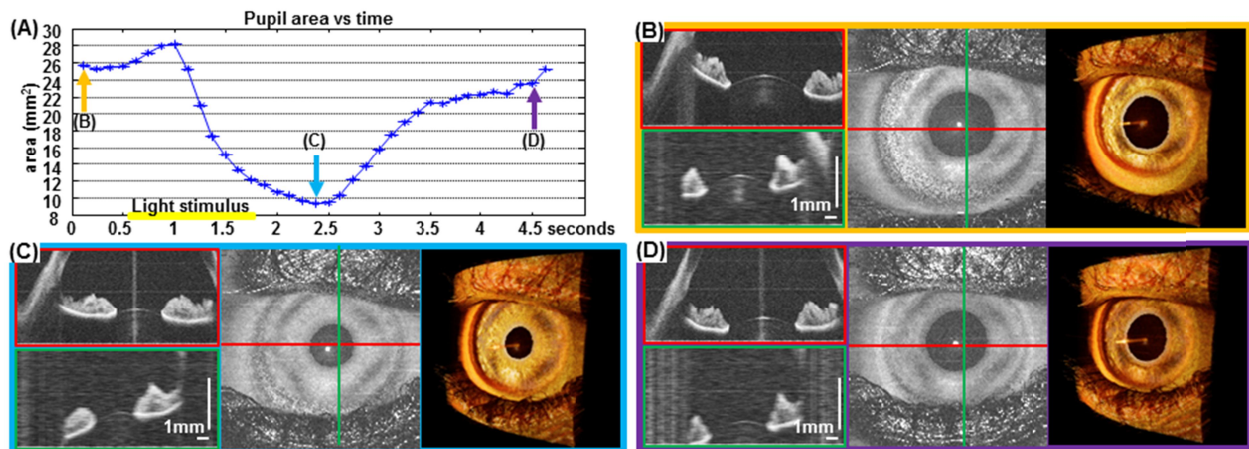
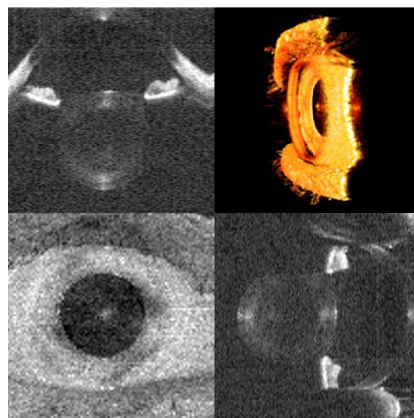


Figure 2. 4-D OCT imaging of the pupillary reflex. (A) Plot of pupil area vs time. (B) Volume#1 at 0.13 seconds. (C) Volume#19 at 2.38 seconds. (D) Volume#38 at 4.5 seconds. The constriction of the iris and the decrease in pupil area is apparent when comparing volume#1 and volume#19. The dilation of the iris and increase in pupil area is visible when comparing volume#19 and volume #38. The cross-sectional OCT images show the iris structure while the enface OCT image depicts the pupil area.

### 3.2 Accommodation dynamics

In the anterior eye, accommodation is the process by which the eye focuses on near objects. This occurs mainly through the deformation of the crystalline lens geometry. Studies of the dynamics of far to near focusing processes may enable understanding several aspects like the age-dependent loss of accommodative amplitude in presbyopia, the development of myopia, and the ageing of the crystalline lens as well as the mechanism of accommodation [9]. We performed 4-D imaging of the focusing process in the anterior eye acquiring 100 x 100 axial-scan volumes over 15mm x 15mm at ~10 volumes per second for 5 seconds at an axial scan rate of 100 kHz (Video 2). The target was moved in position from far to near and the subject was asked to focus on the target and accommodate the target's position change. Two time points are shown from the 4-D data in Figure 3. Pupil diameter decreases when the eye focuses at near positions. The iris becomes smaller while the crystalline lens becomes thicker with surfaces curvature changes.



Video 2. 4-D OCT imaging of the anterior eye focusing on a near object. <http://dx.doi.org/10.1117/12.2004369.2>

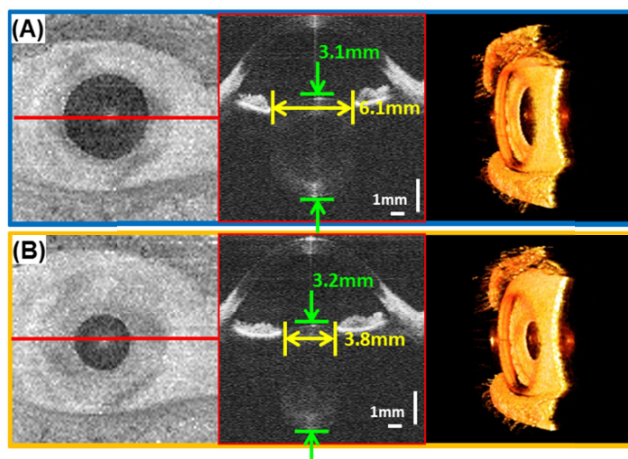


Figure 3. 4-D OCT imaging of the anterior eye focusing on a near object. A) Volume#5 at 0.5 seconds. B) Volume #30 at 3 seconds. The decrease in pupil size and increase in lens thickness is observed and measured.

### 3.3 Tear film break up

The tear film is the first refractive surface for light incident on the eye and plays an important role in the optical quality of the human eye. Tear film dynamics has been used to evaluate the tear system and diagnose dry eye. Tear film break up time (TBUT) is defined as the time interval between a complete blink and the appearance of the first randomly distributed dry spot [10]. A TBUT of less than ten seconds is considered abnormal [11]. Fluorescein dye is typically



used for clinical TBUT measurements. OCT allows for non-invasive tear film dynamics imaging without the need of fluorescein staining. We implemented a 4-D scan protocol with  $300 \times 300$  axial-scan volumes over  $8.5 \text{ mm} \times 8.5 \text{ mm}$  at  $\sim 0.5$  volumes per second for 20 seconds at an axial scan rate of 50 kHz. In order to best visualize tear film break up, we examine the shadowing effect by summing the signal between the anterior surface to the posterior surface of the crystalline lens (Video 3). Tear film break up can be clearly observed in the frame-by-frame breakdown (Figure 4).



Video 3. Illustration of the region of enface summation in a full-eye-length OCT dataset at a single time point for tear film visualization. <http://dx.doi.org/10.1117/12.2004369.3>

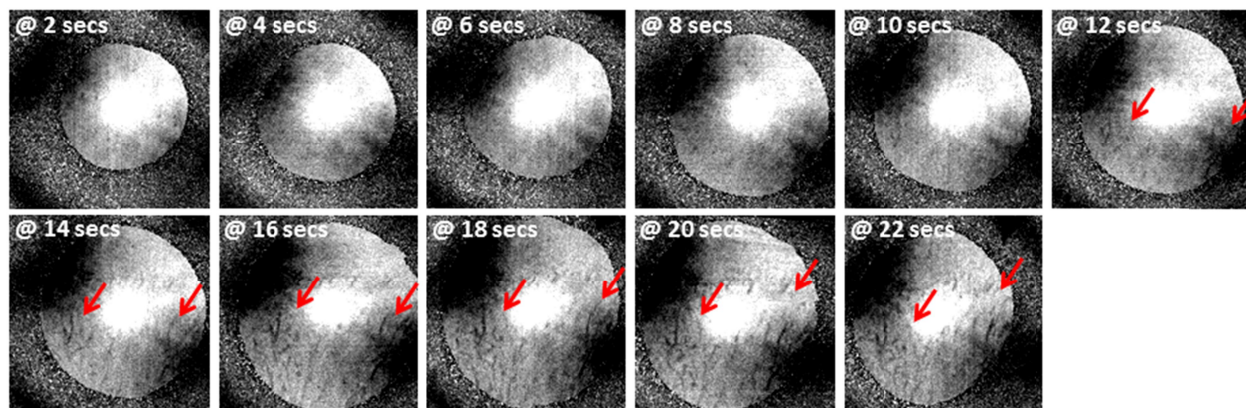
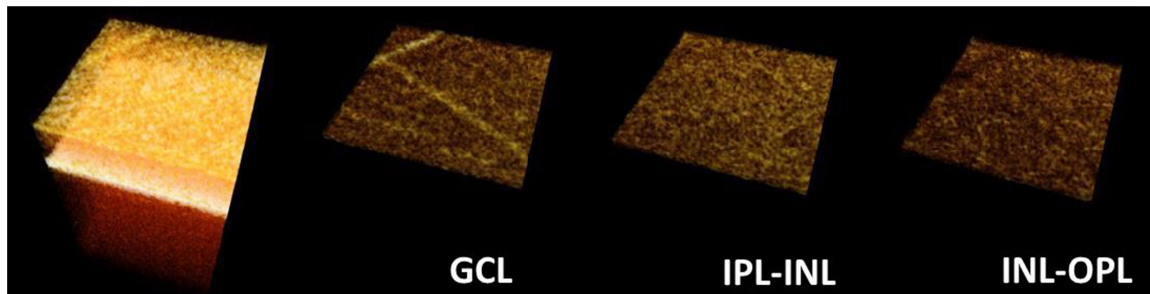


Figure 4. Tear film break up observed in enface images extracted from 4-D OCT data. Tear film break up is observed beginning at  $\sim 12$  seconds where vertical streaking patterns appear.

### 3.4 Retinal blood flow

Retinal blood flow may play a role in the pathogenesis of diseases such as diabetic retinopathy, age-related macular degeneration, and glaucoma. The ability to monitor retinal blood flow may be important not only for treatment, but also for understanding the pathophysiology of these diseases [12-14]. We acquired 4-D data in the retina with  $200 \times 100$  axial-scan volumes over  $1 \text{ mm} \times 0.5 \text{ mm}$  at  $\sim 40$  volumes per second for 1 second at an axial scan rate of 800 kHz (Video 4). Since the galvanometer scanners are driven at very high speeds, a conservative flyback pattern is chosen resulting in only a  $0.5 \text{ mm} \times 0.5 \text{ mm}$  evenly sampled region. Images from a single time point is extracted and shown in Figure 5(B)(C)(D). By taking the variance of maximum intensity projection images at all time points from multiple volumes, we are able to visualize capillaries from the inner to the outer plexiform layers (Figure 5(E)).



Video 4. 4-D OCT imaging of the retina [15]. The video is slowed down 5x with 0.2x playback speed. GCL: ganglion cell layer. IPL-INL: inner plexiform layer to inner nuclear layer. INL-OPL: inner nuclear layer to outer plexiform layer.  
<http://dx.doi.org/10.1117/12.2004369.4>

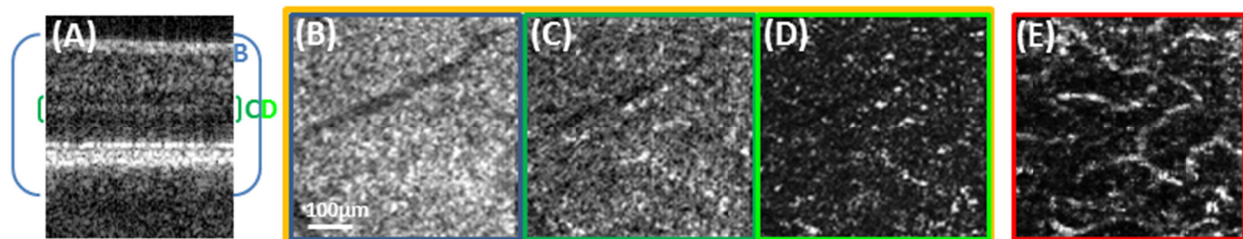


Figure 5. 4-D OCT imaging of retinal blood flow. A) Cross-sectional OCT image. B) Enface summation image in the axial direction of a single volume. C) Enface summation image of a region of interest in the axial direction of a single volume. D) Maximum projection image of a region of interest in the axial direction of a single volume. E) Variance image generated from maximum projection images (like E) of multiple volumes in the 4-D data. The maximum projection image from a single volume shows moving highly reflective scatters. The variance image generated from multiple volumes highlight retinal capillaries.

## 4. CONCLUSIONS

In conclusion, 4-D OCT imaging was demonstrated in the human eye using ultrahigh speed SS-OCT. Visualization and quantitative analysis of 4-D OCT imaging can potentially provide insight to functional and structural changes in the eye with disease. The tunable VCSEL light source enables different imaging modes for variable imaging ranges, speeds, and resolutions. Ultrahigh speed imaging using SS-OCT promises to enable novel 4-D visualization of real-time dynamics of the human eye and may benefit studies by visualizing and characterizing a variety of visual functions.

## ACKNOWLEDGMENTS

The authors want to thank Dr. Al-Hafeez Dhalla, WooJhon Choi, Chen D. Lu, Kathrin J. Molher, and Tsung-Han Tsai at MIT for technical discussions. Financial support from the National Institutes of Health (NIH R01-EY011289-27, R01-EY013178-12, R01-EY013516-09, R01-EY018184-05, R01-EY019029-04, R01-CA075289-14, R01-HL095717-04, R01-NS057476-05), Air Force Office of Scientific Research (AFOSR FA9550-10-1-0063), Medical Free Electron Laser Program (FA9550-10-1-0551) and Deutsche Forschungsgesellschaft (DFG-GSC80-SAOT, DFG-HO-1791/11-1) is gratefully acknowledged. Dr. Ireneusz Grulkowski acknowledges partial support from KOLUMB Fellowship, Foundation for Polish Science (KOL/3/2010-I). Dr. Jay S. Duker is supported by an unrestricted grant from Research to Prevent Blindness as well as the Massachusetts Lions Clubs. Dr. Ireneusz Grulkowski is a visiting scientist from the Institute of Physics, Nicolaus Copernicus University, Torun, Poland.

## REFERENCES

- [1] B. Potsaid, I. Gorczynska, V. J. Srinivasan, Y. Chen, J. Jiang, A. Cable and J. G. Fujimoto, "Ultrahigh speed spectral / Fourier domain OCT ophthalmic imaging at 70,000 to 312,500 axial scans per second," *Opt Express* 16(19), 15149-15169 (2008)
- [2] M. Gora, K. Karnowski, M. Szkulmowski, B. J. Kaluzny, R. Huber, A. Kowalczyk and M. Wojtkowski, "Ultra high-speed swept source OCT imaging of the anterior segment of human eye at 200 kHz with adjustable imaging range," *Opt Express* 17(17), 14880-14894 (2009)
- [3] B. Potsaid, B. Baumann, D. Huang, S. Barry, A. E. Cable, J. S. Schuman, J. S. Duker and J. G. Fujimoto, "Ultrahigh speed 1050nm swept source/Fourier domain OCT retinal and anterior segment imaging at 100,000 to 400,000 axial scans per second," *Opt Express* 18(19), 20029-20048 (2010)
- [4] T. Klein, W. Wieser, C. M. Eigenwillig, B. R. Biedermann and R. Huber, "Megahertz OCT for ultrawide-field retinal imaging with a 1050 nm Fourier domain mode-locked laser," *Opt Express* 19(4), 3044-3062 (2011)
- [5] I. Grulkowski, J. J. Liu, B. Potsaid, V. Jayaraman, C. D. Lu, J. Jiang, A. E. Cable, J. S. Duker and J. G. Fujimoto, "Retinal, anterior segment and full eye imaging using ultrahigh speed swept source OCT with vertical-cavity surface emitting lasers," *Biomed Opt Express* 3(11), 2733-2751 (2012)
- [6] C. K. Leung, C. Y. Cheung, H. Li, S. Dorairaj, C. K. Yiu, A. L. Wong, J. Liebmann, R. Ritch, R. Weinreb and D. S. Lam, "Dynamic analysis of dark-light changes of the anterior chamber angle with anterior segment OCT," *Invest Ophthalmol Vis Sci* 48(9), 4116-4122 (2007)
- [7] C. Y. Cheung, S. Liu, R. N. Weinreb, J. Liu, H. Li, D. Y. Leung, S. Dorairaj, J. Liebmann, R. Ritch, D. S. Lam and C. K. Leung, "Dynamic analysis of iris configuration with anterior segment optical coherence tomography," *Invest Ophthalmol Vis Sci* 51(8), 4040-4046 (2010)
- [8] Y. Lee, K. R. Sung, J. H. Na and J. H. Sun, "Dynamic changes in anterior segment (AS) parameters in eyes with primary angle closure (PAC) and PAC glaucoma and open-angle eyes assessed using AS optical coherence tomography," *Invest Ophthalmol Vis Sci* 53(2), 693-697 (2012)
- [9] M. Ruggeri, S. R. Uhlhorn, C. De Freitas, A. Ho, F. Manns and J. M. Parel, "Imaging and full-length biometry of the eye during accommodation using spectral domain OCT with an optical switch," *Biomed Opt Express* 3(7), 1506-1520 (2012)
- [10] M. A. Lemp and J. R. Hamill, Jr., "Factors affecting tear film breakup in normal eyes," *Arch Ophthalmol* 89(2), 103-105 (1973)
- [11] M. A. Lemp, C. H. Dohlman, T. Kuwabara, F. J. Holly and J. M. Carroll, "Dry eye secondary to mucus deficiency," *Trans Am Acad Ophthalmol Otolaryngol* 75(6), 1223-1227 (1971)
- [12] B. Baumann, B. Potsaid, M. F. Kraus, J. J. Liu, D. Huang, J. Hornegger, A. E. Cable, J. S. Duker and J. G. Fujimoto, "Total retinal blood flow measurement with ultrahigh speed swept source/Fourier domain OCT," *Biomed Opt Express* 2(6), 1539-1552 (2011)
- [13] Y. Jia, O. Tan, J. Tokayer, B. Potsaid, Y. Wang, J. J. Liu, M. F. Kraus, H. Subhash, J. G. Fujimoto, J. Hornegger and D. Huang, "Split-spectrum amplitude-decorrelation angiography with optical coherence tomography," *Opt Express* 20(4), 4710-4725 (2012)
- [14] W. Choi, B. Baumann, J. J. Liu, A. C. Clermont, E. P. Feener, J. S. Duker and J. G. Fujimoto, "Measurement of pulsatile total blood flow in the human and rat retina with ultrahigh speed spectral/Fourier domain OCT," *Biomed Opt Express* 3(5), 1047-1061 (2012)
- [15] T. Schmoll, C. Kolbitsch and R. A. Leitgeb, "Ultra-high-speed volumetric tomography of human retinal blood flow," *Opt Express* 17(5), 4166-4176 (2009)